

Geophysical Research Letters

RESEARCH LETTER

10.1029/2020GL088567

Key Points:

- Trace gas data show southern stratospheric air is getting younger relative to the Northern Hemisphere, in contrast to model predictions
- Both extratropical hemispheres have dynamically driven 5- to 7-year periodicity with large amplitude relative to the age trend
- Multidecadal data sets are required to quantify transport trends that are not confounded by large extratropical variability

Supporting Information:

- Supporting Information S1

Correspondence to:

S. E. Strahan,
 susan.e.strahan@nasa.gov

Citation:












Strahan, S. E., Smale, D., Douglass, A. R., Blumenstock, T., Hannigan, J. W., Hase, F., et al. (2020). Observed hemispheric asymmetry in stratospheric transport trends from 1994 to 2018. *Geophysical Research Letters*, 47, e2020GL088567. <https://doi.org/10.1029/2020GL088567>

Received 23 APR 2020

Accepted 14 AUG 2020

Accepted article online 21 AUG 2020

Observed Hemispheric Asymmetry in Stratospheric Transport Trends From 1994 to 2018

Susan E. Strahan^{1,2} , Dan Smale³ , Anne R. Douglass² , Thomas Blumenstock⁴, James W. Hannigan⁵ , Frank Hase⁴, Nicholas B. Jones⁶ , Emmanuel Mahieu⁷, Justus Notholt⁸ , Luke D. Oman² , Ivan Ortega⁵ , Mathias Palm⁸ , Maxime Prignon⁷ , John Robinson³, Matthias Schneider⁴, Ralf Sussmann⁹, and Voltaire A. Velasco^{6,10} 

¹Universities Space Research Association, Columbia, MD, USA, ²NASA Goddard Space Flight Center, Greenbelt, MD, USA, ³National Institute of Water and Atmospheric Research Ltd., Auckland, New Zealand, ⁴IMK-IFU, Karlsruhe Institute of Technology, Karlsruhe, Germany, ⁵National Center for Atmospheric Research, Boulder, CO, USA, ⁶School of Physics, Wollongong University, Wollongong, New South Wales, Australia, ⁷Institute of Astrophysics and Geophysics, University of Liège, Liège, Belgium, ⁸Institute of Environmental Physics, University of Bremen, Bremen, Germany, ⁹IMK-ASF, Karlsruhe Institute of Technology, Garmisch-Partenkirchen, Germany, ¹⁰Centre for Atmospheric Chemistry, Wollongong University, Wollongong, New South Wales, Australia

Abstract Total columns of the trace gases nitric acid (HNO₃) and hydrogen chloride (HCl) are sensitive to variations in the lower stratospheric age of air, a quantity that describes transport time scales in the stratosphere. Analyses of HNO₃ and HCl columns from the Network for the Detection of Atmospheric Composition Change spanning 77°S to 79°N have detected changes in the extratropical stratospheric transport circulation from 1994 to 2018. The HNO₃ and HCl analyses combined with the age of air from a simulation using the MERRA2 reanalysis show that the Southern Hemisphere lower stratosphere has become 1 month/decade younger relative to the Northern Hemisphere, largely driven by the Southern Hemisphere transport circulation. The analyses reveal multiyear anomalies with a 5- to 7-year period driven by interactions between the circulation and the quasi-biennial oscillation in tropical winds. This hitherto unrecognized variability is large relative to hemispheric transport trends and may bias ozone trend regressions.

Plain Language Summary Our analyses of the 25-year Network for the Detection of Atmospheric Composition Change column HNO₃ and HCl data records from nine stations provide observational evidence that air in the Southern Hemisphere lower stratosphere has been getting younger relative to the Northern Hemisphere at a rate of 1 month/decade since 1994. This stands in contrast to several model studies that predict that Antarctic ozone hole recovery in this century will increase the Southern Hemisphere age of air relative to the Northern Hemisphere. The analyses also reveal extratropical variability with a 5- to 7-year period driven by interactions between the circulation and tropical winds. This previously unrecognized, low-frequency variability is much larger than hemispheric transport trends and is likely to cause bias in trends calculated using data records shorter than about two decades. Understanding and quantifying changes in the transport circulation matters to our ability to model how our protective O₃ layer will evolve in the future.

1. Introduction

The stratospheric ozone (O₃) layer is essential for life on Earth. Ozone-depleting substances (ODSs) are decreasing due to the Montreal Protocol and its amendments (MP), while potent greenhouse gases (GHGs) carbon dioxide (CO₂), nitrous oxide (N₂O), and methane (CH₄) are increasing. Increasing GHGs warm the oceans and drive changes in the stratospheric Brewer-Dobson circulation (BDC) and in the mixing between the tropics and extratropics. Together, the BDC and mixing drive the transport circulation that controls the distributions of ozone and long-lived trace gases such as N₂O and the chlorofluorocarbons (CFCs) (Butchart et al., 2010; Eyring et al., 2007; Oman et al., 2010).

Changes in the stratospheric transport circulation will have far-reaching impacts. The transit time of ODSs to their loss region in the middle and upper stratosphere (Waugh & Hall, 2002) and ODS removal rates through mass exchange with the troposphere (Butchart & Scaife, 2001) are both affected by the transport

circulation. These processes impact ODS lifetimes and the recovery rate of stratospheric ozone. Changes in the stratospheric mass flux of O₃ and long-lived gases into the troposphere will affect chemistry, climate, and surface radiation (Butchart, 2014; Hegglin & Shepherd, 2009; Karpechko & Maycock, 2019). Notably, the persistent influence of stratospheric transport variability on atmospheric composition at the surface was recently identified (Ray et al., 2020). Ray et al. (2020) found that this source of variability must be accounted for in order to correctly estimate ODS emission fluxes, which impacts our ability to accurately assess compliance with the MP (Montzka et al., 2018).

The stratospheric transport circulation can be diagnosed by the age of air (AoA), which is defined as the mean transit time from the Earth's surface to a point in the stratosphere (Waugh & Hall, 2002). Most chemistry climate models (CCMs) predict that the response to increasing GHGs will be cooler stratospheric temperatures, decreased AoA, and an accelerated circulation (Butchart et al., 2010; Oman et al., 2010). Oman et al. (2009) used a suite of CCM simulations to isolate factors affecting AoA and found that increasing sea surface temperatures driven by GHG increases, O₃ depletion and recovery, and the direct radiative effect of GHGs all play a role, but their relative impacts depend on the time period and hemisphere. Recent CCM studies predict that ozone hole recovery this century will counter the impact of GHG increase in the Southern Hemisphere (SH) by causing its AoA to decrease much less than that in the Northern Hemisphere (NH) and decelerate its circulation after 2000 (Abalos et al., 2019; Polvani et al., 2018). Satellite temperature data provide mixed evidence for the predicted circulation change and cannot directly address changes in AoA. Fu et al. (2015) derived an increase in tropical upwelling from temperature trends, indicating that global circulation strengthened (accelerated) from 1980 to 2009, particularly in the SH, which could decrease AoA. However, a later analysis of temperature data from 2000 to 2018 concluded that the global circulation decelerated, with most of the change in the SH (Fu et al., 2019).

AoA trends have been addressed using observations of long-lived trace gases with a known surface trend (Andrews et al., 2001; Engel et al., 2009 & 2017; Schoeberl et al., 2005; Waugh & Hall, 2002). Engel et al. (2017) analyzed 32 CO₂ and SF₆ vertical profiles from 1975 to 2016 and found no significant AoA trend in the northern midlatitude lower and middle stratosphere between 24 and 35 km, but the sparseness of sampling may have precluded any trend detection (Garcia et al., 2011; Waugh, 2009). Analysis of ground-based and satellite measurements of another long-lived trace gas, HCl, supported by a model simulation showed that for a short period, 2007 to 2011, dynamical variability caused AoA and HCl to increase in the NH lower stratosphere (LS), while the opposite occurred in the SH (Mahieu et al., 2014). This suggests that separating a long-term transport trend forced by climate change from short-term dynamical variability requires multidecadal data records.

HNO₃ and HCl are produced from destruction of their long-lived tropospheric sources, N₂O and chlorine-containing halocarbons (e.g., the CFCs) mainly above ~30-km altitude; below that, their distributions are controlled primarily by transport. The columns are most sensitive to the LS transport circulation below ~22 km where more than 70% of their mass resides; see Figure S1 in the supporting information. They are highly correlated with AoA, as well as with N₂O, and each has been used to detect variations in the transport circulation (Douglass et al., 2017; Schoeberl et al., 2005; Strahan et al., 2011; Waugh & Hall, 2002). Fourier transform infrared (FTIR) spectrometers that are part of the Network for the Detection of Atmospheric Composition Change (NDACC, <http://www.ndacc.org>) measure total columns of HNO₃ and HCl at more than 20 stations around the world (De Mazière et al., 2018). To investigate possible multidecadal transport trends, we analyze annual mean anomalies in total column HNO₃ and HCl from all nine extratropical sites that have nearly continuous records of 20 or more years. Because the trace gas column anomalies are highly correlated with LS AoA, we use them as proxies for changes in LS transport. We show that HNO₃ and HCl anomaly trends each provide evidence that the SH transport circulation is getting younger relative to the NH and that most of the change occurs in the SH. In each hemisphere, the trace gas records show multiyear width anomalies with 5- to 7-year periodicity whose amplitude is large relative to the long-term trend, illustrating a major challenge for identifying long-term changes in the transport circulation.

2. Methods, Observations, and Models

The distributions of long-lived trace gases and AoA in the LS are controlled by the combined effects of the BDC and quasi-horizontal mixing across the subtropics, i.e., the transport circulation (Butchart, 2014).

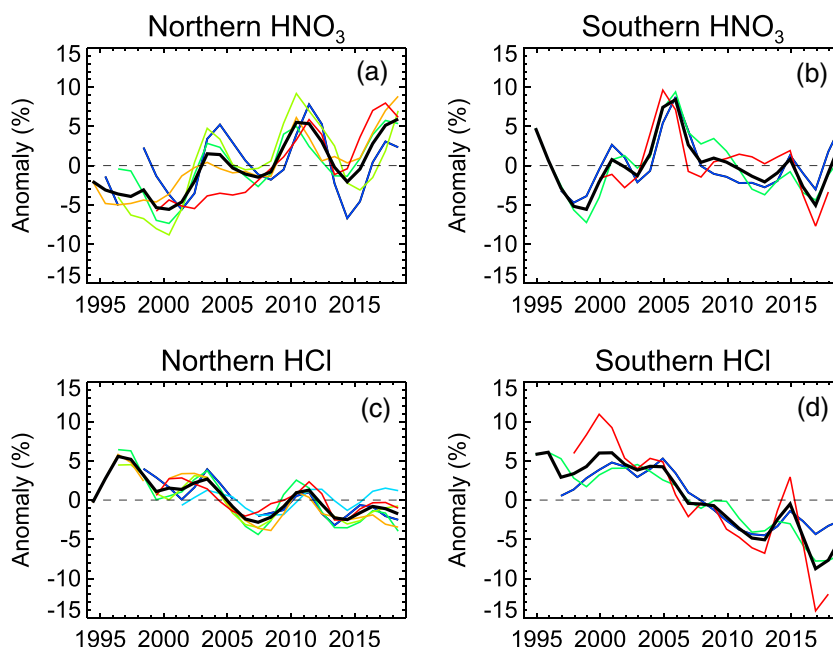


Figure 1. NDACC FTIR annual mean total column anomalies as a percent of each site's long-term mean, 1994–2018, for (a) HNO_3 from five NH sites, (b) HNO_3 from three SH sites, (c) HCl from six NH sites, and (d) HCl from three SH sites. Hemispheric means are shown in black.

The AoA used in this study is calculated with a clock tracer in the Global Modeling Initiative (GMI) chemistry transport model (CTM) integrated with the MERRA2 reanalysis (Gelaro et al., 2017; Strahan et al., 2013). The clock tracer is set to zero at the surface and then ages 1 day per simulated day as it moves through the atmosphere. The correlations between the GMI AoA on model pressure levels and GMI HNO_3 and HCl column anomalies in the extratropics are >0.6 from ~ 30 to 90 hPa, where the highest trace gas number densities are located, with a maximum of 0.9 at the 52-hPa level. See supporting information Figures S1 and S2a.

To examine long-term transport trends, we calculate annual mean HNO_3 and HCl column amounts with measurements from six NH stations $28\text{--}79^\circ\text{N}$ and three SH stations $34\text{--}77^\circ\text{S}$ over the period 1994–2018. FTIR measurements require daylight, and stations poleward of 60° have few or no measurements during winter. For these stations we calculate annual means from late spring through midfall to exclude air that may have been perturbed by heterogeneous chemistry. The supporting information describes the NDACC FTIR measurement network and retrieval methods, the FTIR data sets, and the details of analysis methods. We use the spatial and temporal variability of MERRA2 meteorology manifested in the GMI CTM simulation to extrapolate NDACC FTIR column measurements into zonal and temporal means that reflect all days in a season. This gap-filling method is unaffected by bias in the GMI-simulated column amounts because only the simulated variability, not a column amount, contributes to the extrapolation. This method is helpful when a station is unable to make frequent measurements (i.e., fewer than five measurements per month), for example, due to poor weather or instrument problems. This method and its evaluation are described in the supporting information.

The mean downward motion of the BDC outside the tropics causes HNO_3 and HCl columns to increase with latitude. To compare trends at different latitudes, we normalize each station's record by its long-term mean and then compute annual anomaly percentages. The quasi-biennial oscillation (QBO) is the largest source of variability in the extratropics after the annual cycle, and its variability is mostly but not entirely biennial (Baldwin et al., 2001). In order to identify trends and variability with time scales longer than a QBO cycle, we apply a 3-point binomial (low-pass) filter to the data. The resulting anomaly time series for all stations are shown in Figure 1 along with hemispheric averages. The HNO_3 and HCl anomaly trends seen in Figure 1 include trends from their tropospheric source gases, N_2O and various chlorocarbons; source gas

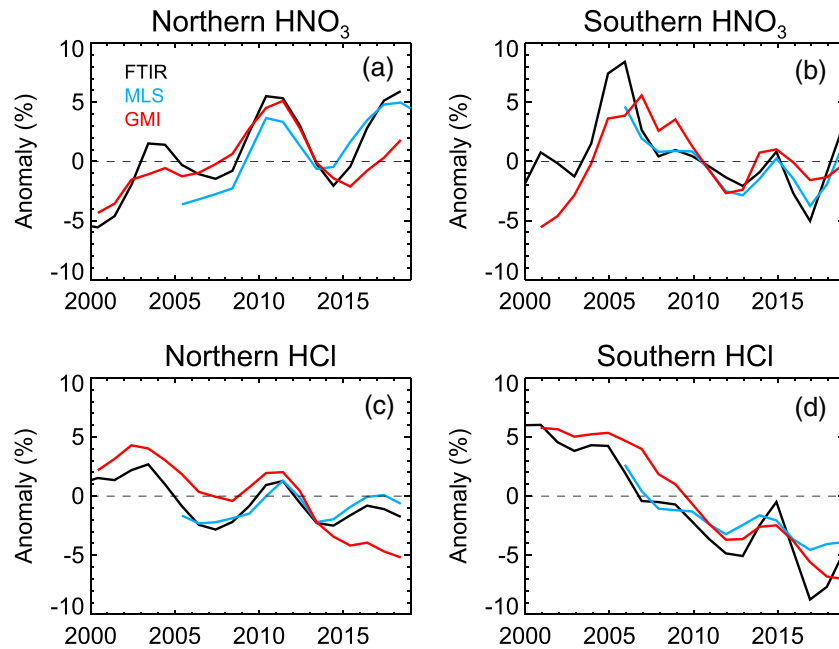


Figure 2. Hemispheric annual mean percentage anomalies from NDACC FTIR measurements (black), MLS satellite data (blue), and the GMI model (red) for (a) NH HNO_3 , (b) SH HNO_3 , (c) NH HCl, and (d) SH HCl. MLS and GMI results are an average over $36\text{--}60^\circ$. MLS stratospheric columns are $215\text{--}0.1$ hPa for HNO_3 and $100\text{--}0.1$ hPa for HCl; GMI results are total columns. All anomalies are calculated with respect to each data set's full length (25 years for NDACC, 14 years for MLS, and 19 years for GMI). MLS anomaly time series are offset between -2 and $+1$ (%) relative to the FTIR time series for ease of comparison. All three records have different long-term means because they have different lengths.

trends will be accounted for later in the analysis of interhemispheric (IH) transport trends. Although there are some outliers, for each species the variability and trends of the anomaly records from all stations within each hemisphere show remarkable similarity.

We also perform the same analysis with midlatitude ($36\text{--}60^\circ$) HNO_3 and HCl stratospheric columns for 2005–2018 from the Aura Microwave Limb Sounder (MLS) (Livesey et al., 2018) and with total columns from the MERRA2 transport circulation in the 1990s (Douglass et al., 2017). The low-pass filtered annual mean anomalies for MLS and the GMI CTM show the same variability and trends as the NDACC analysis (Figure 2). The MLS anomalies are calculated using measurements with near-global daily coverage. The close similarity between the MLS and NDACC results demonstrates that measurements from the nine sites are sufficient to represent changes in the extratropical transport circulation. The NDACC FTIR measurements provide the longest continuous data sets for long-lived stratospheric trace gases, making this network uniquely important for detecting stratospheric transport change.

3. Transport Trends and Variability

3.1. Asymmetry of Southern and Northern Hemisphere Transport Trends

To identify transport circulation change, the contributions from trends in tropospheric source gases, N_2O and various chlorocarbons for HNO_3 and HCl, must be accounted for in the anomaly time series (Figure 1). Source gases enter the stratosphere primarily through the tropical tropopause, and a model simulation confirms that tropospheric trends affect both hemispheres of the stratosphere equally (see supporting information). The impact of source gas trends is eliminated by differencing the SH and NH anomaly time series for each species. The IH anomaly differences, SH – NH, for HNO_3 and HCl have a correlation coefficient (r) of 0.92 and show a clear downward trend in Figure 3. MLS HNO_3 and HCl IH anomalies (blue) show similar trends and variability over the period 2005–2018. The IH difference in the MERRA2 midlatitude AoA (red) closely follows both NDACC anomaly records (black) and indicates that the SH AoA is getting younger

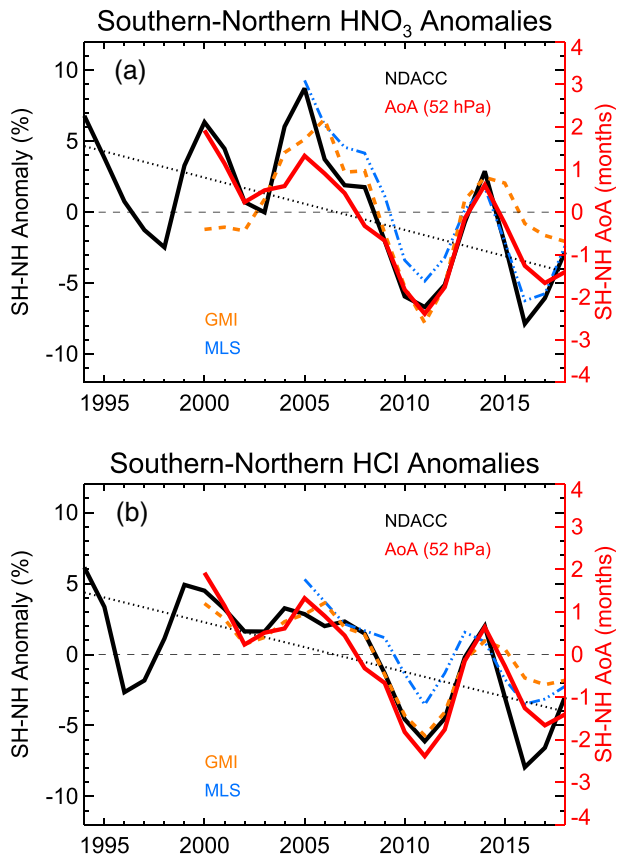


Figure 3. NDACC (black), MLS (blue), and GMI (orange) interhemispheric difference (Southern Hemisphere – Northern Hemisphere) for (a) HNO_3 and (b) HCl anomaly time series. The IH difference of GMI CTM age of air at 52 hPa (red) is plotted in each panel (see the right axis). The dashed line shows the linear trend for the NDACC anomalies. The trends and their uncertainties are reported in Table 1.

from the observed column anomalies. Figures from both studies show that ERA-I and MERRA2 have SH LS midlatitude AoA trending younger relative to the NH. While we find that MERRA2 transport in the GMI CTM does not reproduce the observed trace gas anomaly slopes (i.e., long-term trends) in either hemisphere, we find that it does reproduce the slope and variability of the IH anomaly differences (compare orange and black lines in Figure 3). This close agreement demonstrates that MERRA2 provides reliable information on hemispheric differences in transport and AoA trends, and in their variability between 2000 and 2018.

Trace gas trends for each hemisphere can only be determined after accounting for tropospheric trends in the source gases for HNO_3 and HCl . Accounting for N_2O growth is straightforward because surface mixing ratios have increased at a fairly steady rate of about 0.27%/year for decades (Elkins & Dutton, 2009). Accounting for chlorine decline is more complex because organic chlorine-containing source gases have different lifetimes

relative to the NH. Table 1 reports statistically significant negative trends from a linear fit of the IH differences of the HNO_3 and HCl time series, 1994–2018.

To express the trace gas trends in terms of an LS transport trend, we perform a linear fit of the IH AoA differences at 52 hPa to HNO_3 and to HCl IH anomaly time series; see correlations and fits in supporting information Figure S2b. Applying the fitted slopes and their standard deviations to the fitted trace gas trends, we find the NDACC HNO_3 IH trend corresponds to an IH AoA trend of -0.87 (0.58) month/decade and the NDACC HCl IH trend represents an AoA trend of -1.03 (0.64) month/decade (2 standard deviations in parentheses). The two long-lived column measurements show the same IH transport trend to within their uncertainties. Supporting information Figure S2 shows that AoA/anomaly correlations are >0.8 between 70 and 30 hPa, suggesting that the IH trace gas trends are responding to transport changes in the deep branch of the BDC (i.e., above 70 hPa) (Konopka et al., 2015, and references therein).

Recent studies have found a wide range of climatological AoA values and trends over decadal time scales in different meteorological reanalyses (Chabrillat et al., 2018), so how does using MERRA2 AoA affect the transport trends calculated here? Investigating three reanalyses (MERRA2, ERA-I, and JRA), Ploeger et al. (2019) found robust similarities between seasonal transport and AoA variations, and all showed mainly decreasing AoA from 1989 to 2015. Both studies found that AoA is older in MERRA2 than in the ERA-I or JRA reanalyses, and Ploeger et al. (2019) diagnosed the cause as increased recirculation in the MERRA2 tropical LS, i.e., aging by mixing. They also showed that the fraction of young air in the LS below 500 K (40–50 hPa) was increasing in all three reanalyses although the hemispheric symmetry of the increase differed among them; this will lead to hemispheric differences in their AoA trends. Indeed, Chabrillat et al. (2018) showed differences between NH and SH midlatitude LS AoA trends in five reanalyses during the period analyzed here, suggesting the choice of reanalysis will affect the AoA trends derived

Table 1

Trace Gas Anomaly and AoA Trends in the Extratropical Lower Stratosphere for the Period 1994–2018

Region	HNO_3 (%/year)	HCl (%/year)	AoA from HNO_3 (month/decade)	AoA from HCl (month/decade)
Interhemispheric difference (SH – NH)	-0.37 (0.24)	-0.35 (0.20)	-0.87 (0.58)	-1.03 (0.64)
Southern Hemisphere	-0.28 (0.24)	-0.24 (0.16)	-0.66 (0.58)	-0.70 (0.49)
Northern Hemisphere	0.08 (0.16)	0.10 (0.22)	+0.19 (0.38)	+0.29 (0.64)

Note. Two standard deviations are shown in parentheses. Northern and Southern Hemisphere trends are adjusted to account for source gas trends (see the supporting information). Statistically significant AoA trends are in bold.

and are therefore being removed from the atmosphere at different rates; see the supporting information for details. Using the trace gas anomaly/age relationship determined from the IH analysis above, and after accounting for source gas trends, we find small positive but insignificant trends for HNO_3 and HCl in the NH that represent AoA trends of +0.19 (0.38) and +0.29 (0.64) month/decade, respectively (Figure S4). The SH trends are larger, negative, and significant, corresponding to AoA trends of -0.66 (0.58) and -0.70 (0.49) month/decade for HNO_3 and HCl, respectively. There are two indications that the source gas accounting methods were reasonable: the close agreement between (1) HNO_3 and HCl hemispheric age trends in each hemisphere and (2) the IH trend calculated from the hemispheric trends ($-0.66 - 0.19 = -0.85$ for HNO_3 and $-0.70 - 0.29 = -0.99$ for HCl) and the IH trends determined without applying source gas adjustments (-0.87 and -1.03 , top row of Table 1). However, the uncertainties in the individual hemispheric trends are higher than those in the IH difference trends, which may come from the approximate nature of the source gas accounting. Together, the HNO_3 and HCl trend results in Table 1 show that the SH is getting younger relative to the NH by about 1 month/decade and that this is largely driven by changes in the SH transport circulation.

3.2. Periodic Variability and Trend Detection

A striking feature of the NDACC, MLS, and GMI records in Figure 2 is the ~5- to 7-year period variability with a width of several years whose amplitude is large relative to the long-term trend. The results of several recent studies suggest that this variability is driven not by the QBO directly but by interactions between the BDC annual cycle and the QBO (Ploeger & Birner, 2016; Strahan et al., 2014, 2015). The descending tropical wind regimes of the QBO drive a meridional circulation that creates extratropical composition anomalies during winter and spring that persist until the following winter (Gray & Russell, 1999; Randel & Newman, 1998); circulation and mixing are weak during summer (Orsolini, 2001). Using a CTM simulation integrated with reanalysis meteorology, Ploeger and Birner (2016) showed that the QBO easterly phase at ~22 km (~40 hPa) in the LS shifts the midlatitude AoA spectrum to younger ages. The mean downward motion of the BDC in the extratropics followed by recirculation of the young AoA anomalies back into the tropics allows them to ascend and circulate poleward again. This transport “loop” allows extratropical anomalies to persist 2–3 years, a period that would be present in our analysis after low-pass filtering and consistent with the width of the anomaly peaks and troughs. Strahan et al. (2014) found observational evidence for this pathway in MLS N_2O anomalies that they linked to AoA variations in the SH midlatitudes. In a subsequent study, they showed that positive N_2O anomalies (i.e., younger air) were created during QBO easterly phases that occurred during SH winter (Strahan et al., 2015). Furthermore, these studies identified the occurrence of three QBO easterly phases during SH winter in a 4-year period that created large positive N_2O anomalies in the midlatitudes from 2010 to 2013. This broad positive feature and the large negative N_2O anomalies in 2005 and 2014 (Figure 4a of Strahan et al., 2015) anti-correlate with the SH HNO_3 anomaly structure in Figure 2b. Why this interaction occurs with a 5- to 7-year period is unknown but may be related to the frequency with which the QBO easterly phase descends to a particular altitude and the timing relative to the BDC annual cycle.

The observed large-amplitude, low-frequency variability raises two important issues regarding stratospheric trend detection. The first issue is data record length. MLS data span only two cycles of this variability; thus, its trends depend strongly on the end points. The longer NDACC records show that this is indeed a problem for MLS, as the first full year of measurements, 2005, has the largest positive IH anomaly in the MLS and NDACC records (Figure 3) and will be present but not accounted for in 2005–2018 trends. Other trend studies using shorter satellite data records report hemispheric asymmetry in circulation and AoA trends, e.g., Stiller et al. (2017) and Han et al. (2019), but examination of Figures 2, 3, and S4 places their trends into the context of the longer NDACC record. For example, Figure 3 reveals that the dramatic decrease (increase) in SH (NH) AoA from 2005 to 2012 reported by Stiller et al. (2017) (1) is part of a much longer record of oscillating hemispheric transport strength and (2) coincidentally begins on the peak of a large positive anomaly (2005) and ends near a negative one (2011), which is the largest IH AoA oscillation of the 25-year record. Trends calculated using variable-length NDACC data sets show the fitted IH trend approaches -0.3% to -0.4% per year (-0.7 to -1.1 months per decade) when 21 or more years of data are used, which is roughly four periods of the variability. As the data record length increases, future trend calculations may differ due to periodic variability with time scales greater than those we can detect today.

Acknowledgments

We thank Darryn Waugh and Lorenzo Polvani for thoughtful and stimulating discussions and Megan Damon and Steve Steenrod for integrating GMI simulations. We gratefully acknowledge the NDACC Data Handling Facility for managing the NDACC data product archive. S. E. S. thanks the NASA ACMA and NASA MAP programs for research and model support. Measurements at Lauder and Arrival Heights are core-funded by NIWA through New Zealand's Ministry of Business, Innovation and Employment Strategic Science Investment Fund. D. S. thanks Antarctica New Zealand for providing support for the FTIR measurements at Arrival Heights. The NDACC stations Ny-Ålesund, Izaña, Kiruna, and Zugspitze have been supported by the German Bundesministerium für Wirtschaft und Energie (BMWi) via DLR under grants 50EE1711A, 50EE1711B, and 50EE1711D. T. B. thanks Uwe Raffalski, IRF, for his support of FTIR measurements at IRF Kiruna and Omaira Garcia and Eliezer Sepulveda for their support of FTIR measurements at Izaña Observatory. The National Center for Atmospheric Research is sponsored by the National Science Foundation. The NCAR FTS observation programs at Thule, Greenland, is supported under contract by NASA and by the NSF Office of Polar Programs (OPP). J. W. H. thanks the Danish Meteorological Institute for support at the Thule site. The ULiège contribution to this work has been primarily supported by the Fonds de la Recherche Scientifique—FNRS (F.R.S.–FNRS, Brussels) through the ACCROSS research project (Grant PDR.T.0040.16). E. M. is a research associate at the F.R.S.–FNRS. The long-term monitoring program at the Jungfraujoch station received funding from the F.R.S.–FNRS, the GAW-CH program of MeteoSwiss, and the Fédération Wallonie-Bruxelles. M. P. and J. N. acknowledge the support of the AWI Bremerhaven and of the personnel at the AWIPEV research base in Ny Alesund. We acknowledge the International Foundation High Altitude Research Stations Jungfraujoch and Gornergrat (HFSJG, Bern) for facilities support. N. J. and V. V. wish to acknowledge funding from the Australian Research Council that has supported the FTIR program at the University of Wollongong and recognize colleagues at the Centre for Atmospheric Chemistry for their past and ongoing contributions.

The second issue with low-frequency variations in data records is the accurate regression of variability. In spite of declining ODS levels, Ball et al. (2018) found negative O₃ trends in the NH LS where O₃ has a long lifetime and is controlled by transport. Analytical methods using indices of tropical wind speed and direction to remove QBO variability from trace gas records, e.g., Ball et al. (2018) and Stiller et al. (2012), cannot regress information on periodic variability that has a time scale greater than the longest QBO period (~3 years). But the anomalies shown here and the results from studies noted in section 3.2 indicate that the QBO's interaction with the BDC annual cycle leaves multiyear imprints on midlatitude trace gases. This suggests that standard methods for regressing QBO variability are inadequate for removing the full impact of the QBO on trace gases, which will confound the calculated trend.

4. Conclusions

Understanding the change in the transport circulation, rather than the BDC, is more directly relevant to projecting how O₃ will evolve in the future. The transport circulation directly controls not only the distribution of LS O₃ but also that of key trace gas families inorganic chlorine and odd nitrogen (Cl_y and NO_y) that produce the radicals that control O₃ at all altitudes of the global stratosphere. Our analysis of the 25-year NDACC data records from nine stations provides observational evidence that the southern extratropical LS has been getting younger relative to the NH at a mean rate of 1 month/decade since 1994, with most of the change originating in the SH (~0.7 month/decade). Like Engel et al. (2017), we find a positive but insignificant trend in the NH AoA. The AoA is determined by the BDC and subtropical mixing, so the decrease in SH AoA could mean either increased mixing or increased (accelerated) circulation, or both. The HNO₃ and HCl columns are most sensitive to transport circulation changes at 70 hPa and above, suggesting that the deep branch of the BDC and mixing are affected. The previously noted model studies have predicted that Antarctic ozone hole recovery will slow the GHG-driven decrease in the SH AoA relative to the NH; however, long-lived trace observations show the opposite trend, suggesting that at present, O₃ recovery may not be the dominant influence on the SH transport circulation. Explanation of the observed AoA trends awaits further model investigation and evaluation.

The close similarity between the annual mean anomalies calculated from the NDACC data records and those calculated from MLS observations, which are made daily with near-global coverage, demonstrates that temporally sparse measurements from a ground-based network with a handful of stations in each hemisphere are sufficient to capture changes in the extratropical transport circulation. The continued existence of the NDACC FTIR network is vitally important for the detection of stratospheric climate change.

Conflict of Interest

The authors declare they have no conflicts of interest, financial, or otherwise.

Data Availability Statement

The HNO₃ and HCl FTIR column measurements used in this study are publicly available at <ftp://ftp.cpc.ncep.noaa.gov/ndacc>. Aura MLS data are available at <http://mls.jpl.nasa.gov>. All MERRA2 data sets used here are available from the NASA Goddard Earth Science Data Center (<https://disc.gsfc.nasa.gov/datasets>). The GMI simulation used can be found at <https://portal.nccs.nasa.gov/datashare/dirac/gmidata2/users/mrdamon/Hindcast-Family/HindcastMR2/>.

References

- Abalos, M., Polvani, L., Calvo, N., Kinnison, D., Ploeger, F., Randel, W., & Solomon, S. (2019). New insights on the impact of ozone-depleting substances on the Brewer-Dobson circulation. *Journal of Geophysical Research: Atmospheres*, *124*, 2435–2451. <https://doi.org/10.1029/2018JD029301>
- Andrews, A. E., Boering, K. A., Daube, B. C., Wofsy, S. C., Loewenstein, M., Jost, H., et al. (2001). Mean ages of stratospheric air derived from in situ observations of CO, CH₄, and N₂O. *Journal of Geophysical Research*, *106*(D23), 32,295–32,314. <https://doi.org/10.1029/2001JD000465>
- Baldwin, M. P., Gray, L. J., Dunkerton, T. J., Hamilton, K., Haynes, P. H., Randel, W. J., et al. (2001). The quasi-biennial oscillation. *Reviews of Geophysics*, *39*(2), 179–229. <https://doi.org/10.1029/1999RG000073>
- Ball, W. T., Alsing, J., Mortlock, D. J., Staehelin, J., Haigh, J. D., Peter, T., et al. (2018). Evidence for a continuous decline in lower stratospheric ozone offsetting ozone layer recovery. *Atmospheric Chemistry and Physics*, *18*, 1–15. <https://doi.org/10.5194/acp-18-1379-2018>
- Butchart, N. (2014). The Brewer-Dobson circulation. *Reviews of Geophysics*, *52*, 157–184. <https://doi.org/10.1002/2013RG000448>

- Butchart, N., Cionni, I., Eyring, V., Shepherd, T. G., Waugh, D. W., Akiyoshi, H., et al. (2010). Chemistry–climate model simulations of twenty-first century stratospheric climate and circulation changes. *Journal of Climate*, *23*(20), 5349–5374. <https://doi.org/10.1175/2010JCLI3404.1>
- Butchart, N., & Scaife, A. A. (2001). Removal of chlorofluorocarbons by increased mass exchange between the stratosphere and troposphere in a changing climate. *Nature*, *410*(6830), 799–802. <https://doi.org/10.1038/35071047>
- Chabrilat, S., Vigouroux, C., Christophe, Y., Engel, A., Errera, Q., Minganti, D., et al. (2018). Comparison of mean age of air in five reanalyses using the BASCOE transport model. *Atmospheric Chemistry and Physics*, *18*(19), 14,715–14,735. <https://doi.org/10.5194/acp-18-14715-2018>
- De Mazière, M., Thompson, A. M., Kurylo, M. J., Wild, J. D., Bernhard, G., Blumenstock, T., et al. (2018). The Network for the Detection of Atmospheric Composition Change (NDACC): History, status and perspectives. *Atmospheric Chemistry and Physics*, *18*, 4935–4964. <https://doi.org/10.5194/acp-18-4935-2018>
- Douglass, A. R., Strahan, S. E., Oman, L. D., & Stolarski, R. S. (2017). Multi-decadal records of stratospheric composition and their relationship to stratospheric circulation change. *Atmospheric Chemistry and Physics*, *17*, 12,081–12,096. <https://doi.org/10.5194/acp-17-12081-2017>
- Elkins, J. W., & Dutton, G. S. (2009). Nitrous oxide and sulfur hexafluoride in ‘State of the Climate in 2008’. *Bulletin of the American Meteorological Society*, *90*, S38–S39. <https://doi.org/10.1175/bams-90-8-stateofthecclimate>
- Engel, A., Boenisch, H., Ullrich, M., Sitals, R., Membrive, O., Danis, F., & Crevoisier, C. (2017). Mean age of stratospheric air derived from AirCore observations. *Atmospheric Chemistry and Physics*, *17*, 6825–6838. <https://doi.org/10.5194/acp-17-6825-2017>
- Engel, A., Moebius, T., Boenisch, H., Schmidt, U., Heinz, R., Levin, I., et al. (2009). Age of stratospheric air unchanged within uncertainties over the past 30 years. *Nature Geoscience*, *2*(1), 28–31. <https://doi.org/10.1038/ngeo388>
- Eyring, V., Waugh, D. W., Bodeker, G. E., Cordero, E., Akiyoshi, H., Austin, J., et al. (2007). Multimodel projections of stratospheric ozone in the 21st century. *Journal of Geophysical Research*, *112*, D16303. <https://doi.org/10.1029/2006jd008332>
- Fu, Q., Lin, P., Solomon, S., & Hartmann, D. L. (2015). Observational evidence of strengthening of the Brewer–Dobson circulation since 1980. *Journal of Geophysical Research: Atmospheres*, *120*, 10,214–10,228. <https://doi.org/10.1002/2015jd023657>
- Fu, Q., Solomon, S., Pahlavan, H. A., & Lin, P. (2019). Observed changes in Brewer–Dobson circulation for 1980–2018. *Environmental Research Letters*, *14*, 1–8. <https://doi.org/10.1088/1748-9326/ab4de7>
- Garcia, R. R., Randel, W. J., & Kinnison, D. E. (2011). On the determination of age of air trends from atmospheric trace species. *Journal of the Atmospheric Sciences*, *68*(1), 139–154. <https://doi.org/10.1175/2010JAS3527.1>
- Gelaro, R., McCarty, W., Suarez, M. J., Todling, R., Molod, A., Takacs, L., et al. (2017). The Modern-Era Retrospective Analysis for Research and Applications, version 2 (MERRA-2). *Journal of Climate*, *30*, 5419–5454. <https://doi.org/10.1175/JCLI-D-16-0758.1>
- Gray, L. J., & Russell, J. M. III (1999). Interannual variability of trace gases in the subtropical winter stratosphere. *Journal of the Atmospheric Sciences*, *56*(7), 977–993. [https://doi.org/10.1175/1520-0469\(1999\)056<0977:IVOTGI>2.0.CO;2](https://doi.org/10.1175/1520-0469(1999)056<0977:IVOTGI>2.0.CO;2)
- Han, Y., Tian, W., Chipperfield, M. P., Zhang, J., Wang, F., Sang, W., et al. (2019). Attribution of the hemispheric asymmetries in trends of stratospheric trace gases inferred from Microwave Limb Sounder (MLS) measurements. *Journal of Geophysical Research: Atmospheres*, *124*, 6283–6293. <https://doi.org/10.1029/2018JD029723>
- Hegglin, M., & Shepherd, T. (2009). Large climate-induced changes in ultraviolet index and stratosphere-to-troposphere ozone flux. *Nature Geoscience*, *2*(10), 687–691. <https://doi.org/10.1038/ngeo604>
- Karpechko, A. Y., & Maycock, A. C. (2019). Stratospheric ozone changes and climate In Scientific assessment of ozone depletion: 2018 (Global Ozone Research and Monitoring Project—Report No. 58). World Meteorological Organization.
- Konopka, P., Ploeger, F., Tao, M., Birner, T., & Riese, M. (2015). Hemispheric asymmetries and seasonality of mean age of air in the lower stratosphere: Deep versus shallow branch of the Brewer–Dobson circulation. *Journal of Geophysical Research: Atmospheres*, *120*, 1–14. <https://doi.org/10.1002/2014jd022429>
- Livesey, N. J., Read, W. G., Wagner, P., Froidevaux, L., Lambert, A., Manney, G. L., et al. (2018). Earth Observing System (EOS). Aura Microwave Limb Sounder (MLS). Version 4.2x level 2 data quality and description document (JPL D-33509 Rev D).
- Mahieu, E., Chipperfield, M. P., Notholt, J., Reddmann, T., Anderson, J., Bernath, P. F., et al. (2014). Recent northern hemisphere stratospheric HCl increase due to atmospheric circulation changes. *Nature*, *515*(7525), 104–107. <https://doi.org/10.1038/nature13857>
- Montzka, S. A., Dutton, G. S., Yu, P., Ray, E., Portmann, R. W., Daniel, J. S., et al. (2018). An unexpected and persistent increase in global emissions of ozone-depleting CFC-11. *Nature*, *557*(7705), 413–417. <https://doi.org/10.1038/s41586-018-0106-2>
- Oman, L., Waugh, D. W., Pawson, S., Stolarski, R. S., & Newman, P. A. (2009). On the influence of anthropogenic forcings on changes in the stratospheric mean age. *Journal of Geophysical Research*, *114*, D03105. <https://doi.org/10.1029/2008jd010378>
- Oman, L. D., Plummer, D. A., Waugh, D. W., Austin, J., Scinocca, J. F., Douglass, A. R., et al. (2010). Multimodel assessment of the factors driving stratospheric ozone evolution over the 21st century. *Journal of Geophysical Research*, *115*, 1–21. <https://doi.org/10.1029/2010jd014362>
- Orsolini, Y. J. (2001). Long-lived tracer patterns in the summer polar stratosphere. *Geophysical Research Letters*, *28*(20), 3855–3858. <https://doi.org/10.1029/2001GL013103>
- Ploeger, F., & Birner, T. (2016). T. Seasonal and inter-annual variability of lower stratospheric age of air spectra. *Atmospheric Chemistry and Physics*, *16*, 10,195–10,213. <https://doi.org/10.5194/acp-16-10195-2016>
- Ploeger, F., Legras, B., Charlesworth, E., Yan, X., Diallo, M., Konopka, P., et al. (2019). How robust are stratospheric age of air trends from different reanalyses? *Atmospheric Chemistry and Physics*, 6085–6105.
- Polvani, L. M., Abalos, M., Garcia, R., Kinnison, D., & Randel, W. J. (2018). Significant weakening of Brewer–Dobson circulation trends over the 21st century as a consequence of the Montreal Protocol. *Geophysical Research Letters*, *45*, 401–409. <https://doi.org/10.1002/2017GL075345>
- Randel, W. J., & Newman, P. A. (1998). The stratosphere in the southern hemisphere. In D. J. Karoly, & D. G. Vincent (Eds.), *Meteorology of the Southern Hemisphere* (pp. 243–282). Boston, MA: American Meteorological Society.
- Ray, E., Portmann, R. W., Yu, P., Daniel, J., Montzka, S. A., Dutton, G. S., et al. (2020). The influence of the stratospheric quasi-biennial oscillation on trace gas levels at the Earth’s surface. *Nature Geoscience*, *13*(1), 22–27. <https://doi.org/10.1038/s41561-019-0507-3>
- Schoeberl, M. R., Douglass, A. R., Polansky, B., Boone, C., Walker, K. A., & Bernath, P. (2005). Estimation of stratospheric age spectrum from chemical tracers. *Journal of Geophysical Research*, *110*, D21303. <https://doi.org/10.1029/2005jd006125>
- Stiller, G. P., Fierli, F., Ploeger, F., Cagnazzo, C., Funke, B., Haenel, F. J., et al. (2017). Shift of subtropical transport barriers explains observed hemispheric asymmetry of decadal trends of age of air. *Atmospheric Chemistry and Physics*, *17*, 11,177–11,192. <https://doi.org/10.5194/acp-17-11177-2017>

- Stiller, G. P., von Clarmann, T., Haenel, F., Funke, B., Glatthor, N., Grabowski, U., et al. (2012). Observed temporal evolution of global mean age of stratospheric air for the 2002 to 2010 period. *Atmospheric Chemistry and Physics*, *12*(7), 3311–3331. <https://doi.org/10.5194/acp-12-3311-2012>
- Strahan, S. E., Douglass, A. R., & Newman, P. A. (2013). The contributions of chemistry and transport to low Arctic ozone in March 2011 derived from Aura MLS observations. *Journal of Geophysical Research: Atmospheres*, *118*, 1563–1576. <https://doi.org/10.1002/jgrd.50181>
- Strahan, S. E., Douglass, A. R., Newman, P. A., & Steenrod, S. D. (2014). Inorganic chlorine variability in the Antarctic vortex and implications for ozone recovery. *Journal of Geophysical Research: Atmospheres*, *119*, 14,098–14,109. <https://doi.org/10.1002/2014JD022295>
- Strahan, S. E., Douglass, A. R., Stolarski, R. S., Akiyoshi, H., Bekki, S., Braesicke, P., et al. (2011). Using transport diagnostics to understand chemistry climate model ozone simulations. *Journal of Geophysical Research*, *116*, D17302. <https://doi.org/10.1029/2010jd015360>
- Strahan, S. E., Oman, L. D., Douglass, A. R., & Coy, L. (2015). Modulation of Antarctic vortex composition by the quasi-biennial oscillation. *Geophysical Research Letters*, *42*, 4216–4223. <https://doi.org/10.1002/2015GL063759>
- Waugh, D. (2009). Atmospheric dynamics: The age of stratospheric air. *Nature Geoscience*, *2*(1), 14–16. <https://doi.org/10.1038/ngeo397>
- Waugh, D. W., & Hall, T. M. (2002). Age of stratospheric air: Theory, observations and models. *Reviews of Geophysics*, *40*(4), 1010. <https://doi.org/10.1029/2000rg000101>

References From the Supporting Information

- Aquila, V., Oman, L. D., Stolarski, R., Douglass, A. R., & Newman, P. A. (2013). The response of ozone and nitrogen dioxide to the eruption of Mt. Pinatubo at southern and northern midlatitudes. *Journal of the Atmospheric Sciences*, *70*(3), 894–900. <https://doi.org/10.1175/JAS-D-12-0143.1>
- Bosilovich, M. G., Akella, S., Coy, L., Cullather, R., Draper, C., Gelaro, R., et al. (2015). MERRA-2: Initial evaluation of the climate. NASA Technical Report Series on Global Modeling and Data Assimilation. (NASA/TM-2015-104606, Vol. 43).
- Hase, F., Blumenstock, T., & Paton-Walsh, C. (1999). Analysis of the instrumental line shape of high-resolution Fourier transform IR spectrometers with gas cell measurements and new retrieval software. *Applied Optics*, *38*(15), 3417–3422. <https://doi.org/10.1364/AO.38.003417>
- Hase, F., Hannigan, J. W., Coffey, M. T., Goldman, A., Höpfner, M., Jones, N. B., & Wood, S. W. (2004). Intercomparison of retrieval codes used for the analysis of high-resolution, groundbased FTIR measurements. *Journal of Quantitative Spectroscopy and Radiative Transfer*, *7*, 25–52. <https://doi.org/10.1016/j.jqsrt.2003.12.008>
- Kohlhepp, R., Ruhnke, R., Chipperfield, M. P., De Maziere, M., Notholt, J., Barthlott, S., et al. (2012). Observed and simulated time evolution of HCl, ClONO₂, and HF total column abundances. *Atmospheric Chemistry and Physics*, *12*(7), 3527–3556. <https://doi.org/10.5194/acp-12-3527-2012>
- Kremser, S., Thomason, L. W., von Hobe, M., Hermann, M., Deshler, T., Timmreck, C., et al. (2016). Stratospheric aerosol—Observations, processes, and impact on climate. *Reviews of Geophysics*, *54*, 278–335. <https://doi.org/10.1002/2015RG000511>
- Pougatchev, N. S., Connor, B. J., & Rinsland, C. P. (1995). Infrared measurements of the ozone vertical distribution above Kitt Peak. *Journal of Geophysical Research*, *100*(D8), 16,689–16,697. <https://doi.org/10.1029/95JD01296>
- Rodgers, C. D. (2000). *Inverse methods for atmospheric sounding—Theory and practice, Series on Atmospheric Oceanic and Planetary Physics* (Vol. 2). London: World Scientific Publishing Co. Pte. Ltd. <https://doi.org/10.1142/3171>
- Ronsmans, G., Langerock, B., Wespes, C., Hannigan, J. W., Hase, H., Kerzenmacher, T., et al. (2016). First characterization and validation of FORLI-HNO₃ vertical profiles retrieved from IASI/Metop. *Atmospheric Measurement Techniques*, *9*, 4783–4801. <https://doi.org/10.5194/amt-9-4783-2016>